Superelastic conductor material with enhanced fatigue durability for implantable lead service

Jeremy E Schaffer, Adam J Griebel, Drew J Forbes, Ross Wood, Lisa Powell, Dave Braaten, Song Cai

Abstract

Implantable biostimulation leads provide critical electrical conduits for cardiostimulation and neurostimulation devices. These leads are highly engineered wire constructs which must withstand many years of flexural motion and consequently require high fatigue resistance. This study proposes and demonstrates a new wire construct concept which offers a step-change improvement in fatigue resistance. Wire constructs with a high conductivity silver core are characterized in a form factor that aligns with conductor subcomponents commonly used in leads. Nitinol is effectively substituted for 35N LT® (CoNiCrMo) and shown to give 50 to 100% improvements in cyclic strain-loading fatigue performance for bifilar coils or monofilament wire respectively in a lab bench test at body temperature (310K ± 2). Electrical isolation of polyimide coating of the nitinol-based conductors is visually maintained in the 2-channel coils even after high temperature (450-550°C) secondary shape setting. While the ultimate strength of the nitinol-silver composite wire (NiTi-DFT®-30Ag) at about 1000 MPa was lower than 35NLT-silver composite wire (35NLT-DFT-28Ag) at about 1600 MPa, the work energy to tensile fracture was 65.9 mJ/mm^3 for NiTi-DFT-30Ag and 23.7 mJ/mm^3 for 35NLT-DFT-28Ag, requiring significantly more work energy to overload the nitinol-based conductor.

Introduction

Since the first cardiac pacemaker implantation in 1960, these lifesaving devices have improved dramatically in capability, longevity, and reliability. The devices generally comprise two primary components: a pulse generator and one or more leads. Pulse generators comprise a battery and small computer in a hermetically sealed housing; their size often necessitates implantation some distance from the heart. The leads, complex assemblies of highly engineered wires and polymers, are used to transmit electrical signals to and from the generator and the heart tissue. Improvements in generator and lead technology combined with widespread adoption of cardiac pacemakers led to the commercialization of additional device types including implantable cardioverter defibrillators (ICD's), deep brain stimulators (DBS) and spinal cord and peripheral nerve stimulators [1, 2]. As these leads often need to function continuously for decades and can see hundreds of millions and even billions of cycles of flexural motion, fatigue resistance is a key design requirement [3].

Lead fatigue resistance is a function of construct geometry, material selection, and wire processing. It is important to note that strain fatigue and not stress fatigue is the primary concern; leads are generally not mechanically functional and so simply need to move with the surrounding tissue without sustaining damage. Geometric configuration is the first line of defense against fatigue damage where incorporation of fine wires into strand, cable, or coil configurations reduces the maximum strain experienced by any individual wire. Proper wire alloy selection is also key. Some of the earliest pacing leads were produced with Drawn Brazed Strand (DBS®) composite wires containing 316L stainless steel wires disposed around and brazed to a silver core [4]. In the 1980's, a new type of composite wire known as a DFT® (drawn filled tube) wire was introduced by Fort Wayne Metals, comprising a MP35N shell around a silver core. While

fatigue resistance of these MP35N wires was good, titanium-nitride inclusions limited the fatigue life. 35N LT®, with low titanium content, was later introduced to reduce these inclusions and substantially improved the fatigue resistance of the wires and thereby pacing leads [5]. 35N LT and 35NLT-DFT-Ag (designating a shell of 35N LT and a core of Ag) are now the dominant wire materials used in biostimulation leads today and have a proven record of performance [6, 7]. A specially processed variant of 35N LT with a nanocrystalline microstructure (NDR®) and subsequent enhanced fatigue resistance has been more recently introduced and found utility in especially demanding lead applications [8]. While the biostimulation leads in use today are well-served by 35N LT, materials with improved fatigue resistance would extend minimum service lifetimes and enable new indications and designs. Figure 1 shows unpublished fatigue strain-life data taken from Ø 0.18 mm wires that were processed using industrial medical wire standards and provides an empirical illustration of advancing strain fatigue resistance of lead materials.

A casual review of common medical alloys and their strain-fatigue properties reveals one material which surpasses most others: Nitinol. An intermetallic compound of nickel and titanium, nitinol offers low stiffness, high strength, and a unique ability to elastically recover deformations exceeding 10% strain (superelasticity). These properties have led to widespread use in guidewires and peripheral, neurovascular, and gastrointestinal stenting. The low stiffness of nitinol drives relatively low stresses for a given strain level, and the superelasticity, whether transformational or linear elastic, can make the component tolerant of extreme displacements. Nitinol wire often possesses double the strain-fatigue strength of 35N LT (Figure 1). However, nitinol is seldom used in leads today.

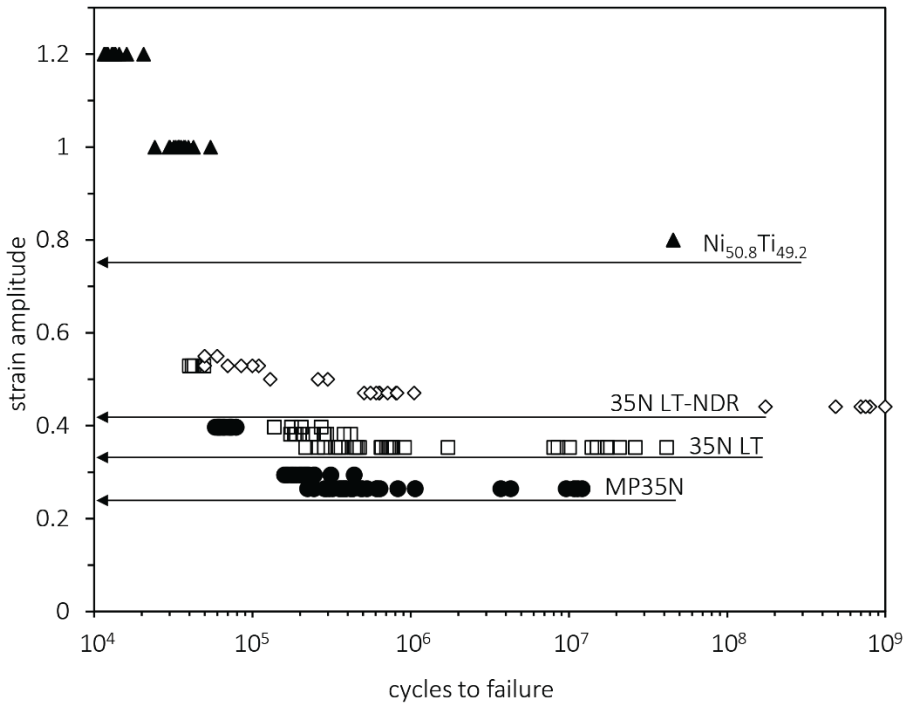

Figure 1. Unpublished rotating beam fatigue (R = -1) test data for Ø 0.18 mm wires of spring temper MP35N, 35N LT, 35N LT-NDR (nanocrystalline), and superelastic nitinol (Ni50.8Ti49.2) wire tested in RO water at 60 Hz and 310K [9].

The lack of nitinol-based leads can be attributed to two factors. First, the cobalt based MP35N and 35N LT materials have generally performed well for decades, and there is substantial industrial and regulatory inertia behind their use. Second, nitinol's elasticity and requisite heat treatments complicate the manufacture of coil constructs. One common lead design employs a bifilar coil, where each filar of the coil is electrically insulated from the other by first coating the wires with a polymer. These coated wires are wound around a mandrel, and plastic deformation gives stability to the coil shape. This technique works well for 35N LT, but the elasticity of nitinol complicates coil forming via plastic deformation. Nitinol requires a heat treatment, generally 300-500°C, to "shape set" the wire and impart functional properties. Typical polymers like ETFE cannot withstand these temperatures. To widely implement nitinol in coil-based leads, an alternative polymer is needed. Polyimide enamels offer excellent thermal stability and electrical resistance and are used in many medical devices today. Importantly, polyimide can withstand the temperatures needed to shape set nitinol, potentially enabling nitinol coil-based leads.

If nitinol could be readily employed in biostimulation lead constructs, it could enable new and enhanced device designs. For example, future pacing and defibrillation design paradigms may include hybrid systems incorporating implantable wireless pulse generators exterior to the heart with short transmyocardial leads. Such hybrid systems could take advantage of seed-sized leadless appliances without consuming precious internal atrial or ventricular chamber real estate, especially in younger device recipients that may require repeat implantation [10]. Such heart wall-crossing leads would necessarily require high myocardial compliance matching while maintaining electrical integrity through hundreds of millions of cycles of implant life [10]. Better compliance matching with high backbone strength and enhanced cyclic displacive durability may also help mitigate rare lead fracture issues near suture anchor points and difficult anatomical geometries found in conventional lead uses [11, 12].

A deployable lead system with programmable shape set features common to nitinol stents may also provide clinical fixation benefit. For example, passive anchoring of some leads is accomplished today by creating wave or helical features that create gentle vessel apposition, as for example in the coronary sinus for cardiac resynchronization therapy [13]. A nitinol-based lead system with the right choice of thermally stable polymers could be programmed to a deployable shape beneficial to gentle vessel or tissue anchor purposes providing gentle delivery, stable anchoring and simplified retrieval compared to active fixation.

The aim of this study was to demonstrate the feasibility and performance of nitinol-based wire constructs for biostimulation lead design. Prototype NiTi-DFT-Ag composites were fabricated and compared to the clinically familiar 35NLT-DFT-Ag composite wires in terms of tensile, fatigue, and electrical behavior in wire, coil, and cable form.

Materials

Wire Production

Reference composite wire with a 35N LT® shell and pure silver (99.99% purity) core was produced by precision machining shell material to a tubular form, conditioning the material to provide smooth surfaces free from contamination and debris, then filling the tubular materials with high purity silver and co-processing to form silver-core monofilament DFT (drawn filled tube) wires. In this study, the silver core comprised 28% of the cross-sectional area of the wire, and this composite is designated as 35NLT-DFT-28Ag. The cold reduction and annealing processes were conducted using diamond die draw practices and reel-to-reel tubular furnaces by conventional means as published elsewhere [14, 7].

The experimental composite wire with a nitinol shell and pure silver core was produced in a similar manner as described above. For the experimental wire, the core percentage was slightly larger at 30% but still within typical tolerances. This composite is designated as NiTi-DFT-30Ag. Nitinol used here was $Ni_{50.8}Ti_{49.2}$ (at.%) extra low interstitial grade material with an ingot austenitic peak temperature (Ap) of 248 K (SE508 ELI grade, Confluent Medical, Scottsdale, AZ) as defined by ASTM F2004-17.

Both composite wire materials were processed down to testable configurations given in Table 1, where bifilar coils are denoted as 2 wires x 0.100 mm coated with polymer and coiled to 0.76 mm OD and strands are given as 1 x 19, as in: 19 concentrically wound filaments of 0.025 mm wire with a nominal OD of 0.125 mm.

Table 1. Wire-based DFT® wire constructs assessed in this study.

Wire	Material	Type	Size/Configuration
1 2	35N LT-DFT-28%Ag NiTi-DFT-30%Ag	Monofilament wire	0.100 mm
3 4	35N LT-DFT-28%Ag NiTi-DFT-30%Ag	1x19 Stranded wire	1x19x0.025; 0.125 mm
5	35N LT-DFT-28%Ag	ETFE-coated Bifilar coiled wire	2 x 0.100/0.147; 0.76 mm
6	NiTi-DFT-30%Ag	Polyimide-coated Bifilar coiled wire	2 x 0.100/0.114; 0.76 mm

Coatings

Ethylene tetrafluoroethylene (ETFE) was applied by crosshead extrusion over 0.100 mm Wire 1 to achieve a total diameter of 0.147 mm giving a polymer wall thickness of 24 microns. Pyre-M.L. (RC5019, Industrial Summit Technology, Otsu, Japan) polyimide (PI) enamel was applied, and heat cured layer-by-layer to achieve a coated diameter of 0.114 mm over 0.100 mm Wire 2 giving a polymer wall thickness of 7 microns.

Bifilar Coils

Bifilar (2-wire) coils of both 0.1 mm coated 35NLT-DFT-28Ag and NiTi-DFT-30Ag were formed using tubular strand equipment to form to a final OD of 0.76 mm. 35NLT-DFT-28Ag was cold-formed to the mandrel and removed as a stable coil (Wire 5) without using heat to stabilize the shape. NiTi-DFT-30Ag coils (Wire 6) required heating to about 773 K for seconds to stress relieve the nitinol, reverting the SMA backbone from strained martensite (as-coiled) to austenite parent phase, thereby shape setting the coiled form prior to mandrel removal. Figure 2 shows the surface and cross-sections of polyimide-coated, strand-coiled and shape set DFT Wire 6 in (a) secondary electron imaging of the coated coil surface; (b) a singular wire section showing the distinct wire ingredients; and (c) multiple sections of coil elements with adjacent-wire polymer isolation after complete thermal processing.

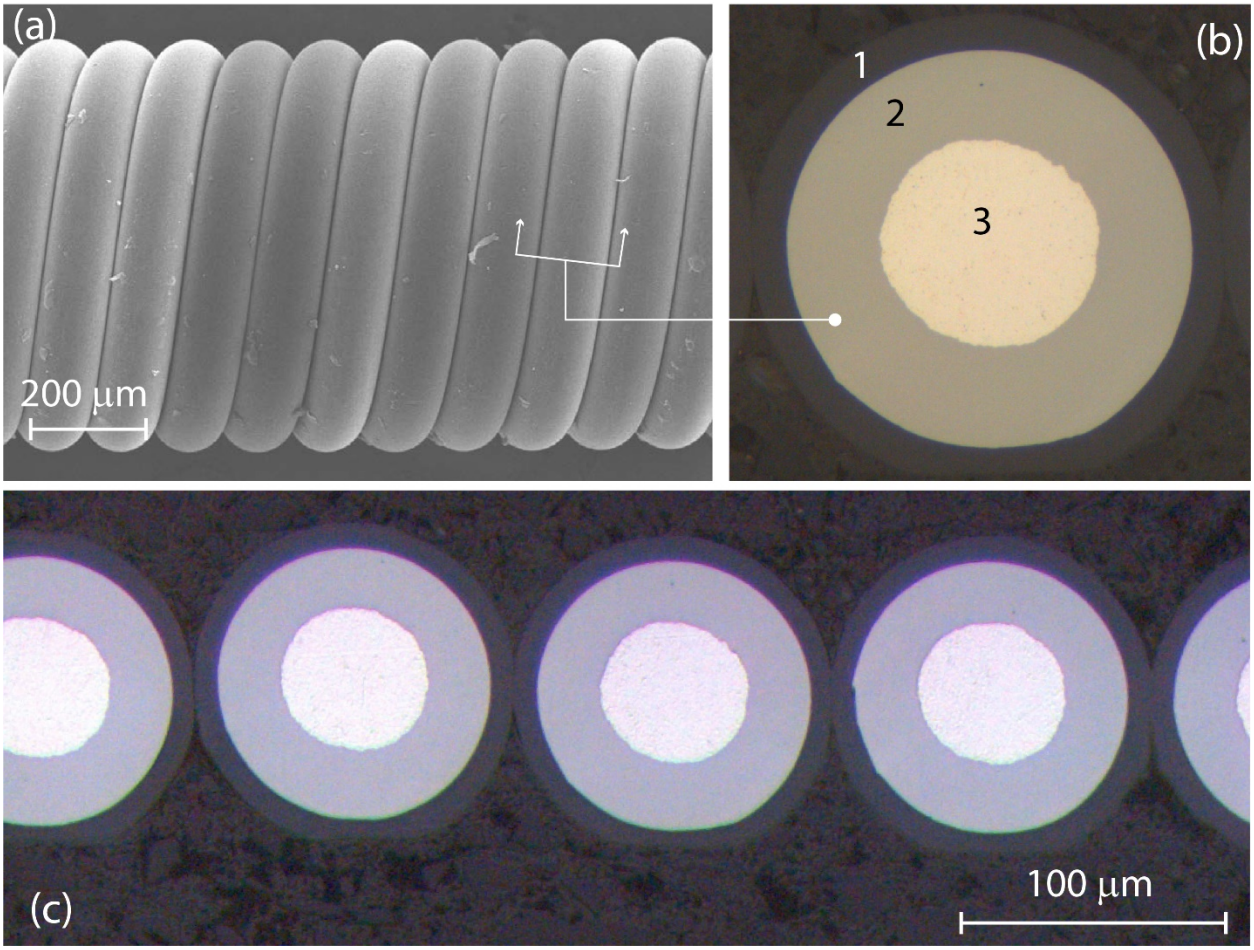

Figure 2 – Example bifilar coil image and coiled wire cross-sections of NiTi-DFT-30Ag (Wire 6) with representative secondary electron SEM image (a) and cross-sectional images in (b and c) showing the PI coating (1), the superelastic nitinol mechanical backbone (2), and the high purity, high conductivity 99.99% silver core element (3); serial elements are shown in (c) sectioned from the coil after polyimide coating, stranding and shape set heat treatment.

Strands

Figure 3 shows metallographically prepared cross-sections of the nineteen by 25 μm DFT®-wire strands with total outside diameters of about 125 μm. The chosen concentric strand configuration is representative of conductors used in some neurological and cardiac stimulation leads and were produced as concentric 1x19 configurations in both 35NLT-DFT-28Ag (Wire 3) and NiTi-DFT-30Ag (Wire 4). In both configurations, monofilament 25 μm wires were concentrically stranded first six over one, and then 12 over 7 wires to give 18 helixed conductor wires around one straight core element as shown in Figure 3. Both strand types were thermally stress relieved for seconds at 773 to 973 K using a reel-to-reel process to stabilize the multifilament wires against fray at cut ends.

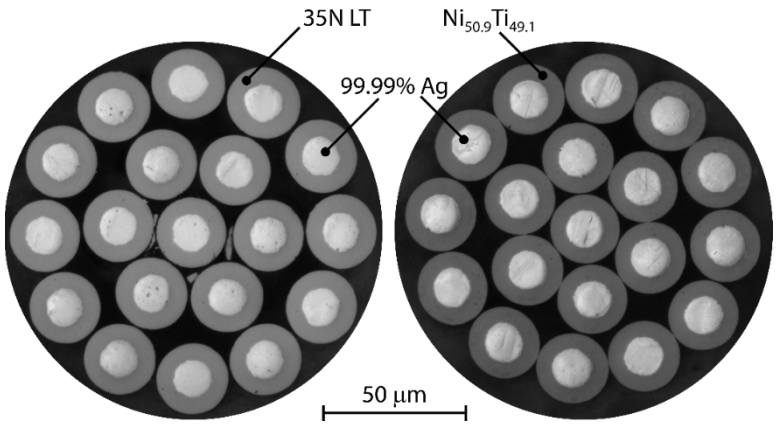

Figure 3 – Cross-sections of Wire 3, 35NLT-DFT-28Ag (left), and Wire 4, NiTi-DFT-30Ag (right) 19-wire multifilament composite strands, a strand geometry found in some implantable neural lead systems.

Methods

Tensile testing was conducted in accordance with standard ASTM E8 / E8M – 21 using an Instron 5565 tensile test frame. Monotonic uniaxial tensile properties were measured for each material at 298 K at a strain rate of 10^{-3} s-1 with pneumatic grips and flat grip faces lined with fine 600-grit emery to prevent sample slippage.

Wire resistance testing was performed using a temperature-compensated 4176 Precision Micro-Ohmmeter (Valhalla Scientific) to assess direct current (DC) resistance over a 304.8 mm straight wire section. Diameters for use in resistance and tensile stress calculations were measured using a high precision bench micrometer equipped with a Dorsey gage (0.00005 inch graduations, Dorsey Metrology International and 673MXZ bench micrometer, L.S. Starrett Co).

Rotary beam fatigue testing in accordance with ASTM E2948 was conducted on 0.1 mm Wires 1 and 2 to assess basic material level fatigue life. Fatigue life was assessed at various strain loads using equipment manufactured by Positool, Inc. at 60 Hz in body temperature 310K (± 2) 0.9% saline with a strain load ratio of R = -1. The monofilament specimens were tested at alternating strain levels ranging from 0.5 to 2.5% to fracture or to a runout criterion of 10^8 cycles.

Coil flexural fatigue testing of Wires 5 and 6 was attempted by rotary beam methods using the same Positool rotating chuck apparatus. In this test, the minimum free-loop chuck and rest geometry governed the maximum achievable outer fiber wire alternating strain to about 0.40%. Under this strain-load level at 60 Hz in body temperature saline, neither coil configuration fractured over 10 samples within the 10^8 cycle runout criteria and tensile-tensile fatigue testing was commenced to induce a more severe material strain condition.

Coil tensile-tensile fatigue testing was performed using 3.5 mm discrete specimens of Wires 5 and 6 loaded in body temperature distilled water on a Bose Enduratec ELF 3230 system (TA Instruments, Eden Prairie, MN) with custom wire grip, continuity, and load sensing (Element Minneapolis, Minnetonka, MN). Compliant sections of coated bi-filar material were formed at a gage length of 3.5 mm with continuous stretched support sections for electrical tape padding (Fig. 4a) before loading into flat face steel grips (Fig. 4b) and further loading into the distilled-water-immersed fatigue system (Fig. 4c) with 6 parallel samples per test setup. All fixtured parts and grips were aligned and secured before final loading and cycling at a

rate of 35 Hz at a bath temperature of 310K (± 2). Displacement conditions for cycling were 7 mm mean displacement and levels of ± 0.35, ± 0.53 and ± 0.75 mm giving structural strains of 200% mean and alternating structural strains of 10%, 15% and 21.4% respectively. Specimens were cycled until fracture or a 10^8-cycle runout criterion.

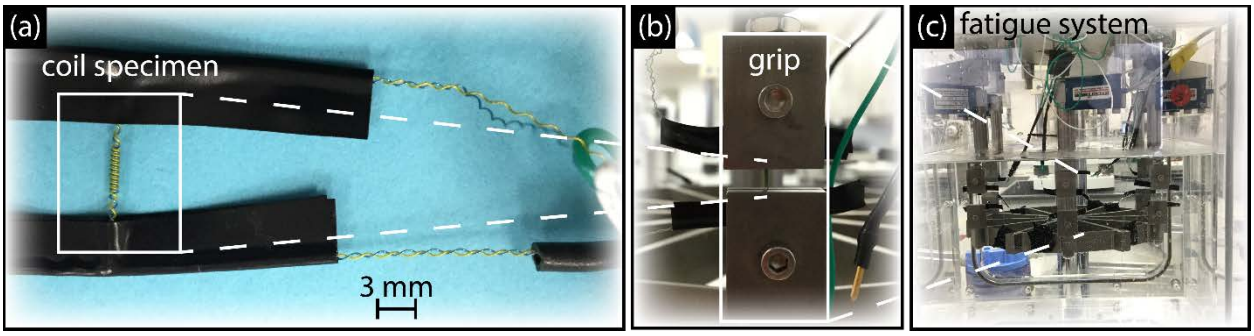

Figure 4 – Coil tension-tension fatigue setup comprising: (a) 3.5 mm length bifilar coil specimen ready for loading to rigid grips and electrical continuity test unit; (b) rigid steel grips clamped with electrical lead connections; and (c) the distilled water immersed 12 specimen fatigue system loaded with 6 fatigue specimens ready for cycling at 35 Hz and T = 310K (± 2).

Results

Figure 5 shows the tensile behavior of Ø 0.1 mm monofilament and Ø 0.125 mm 19-wire strands of both nitinol- and 35N LT-based materials. An ultimate strength and elongation to fracture of about 1600 MPa and 2.8% strain respectively was observed for Wire 1, on par with similar wires used in the medical device industry. In stranded form (Fig. 5c), Wire 3 was measured at about 90% of the strength and elongation of monofilament wire (Fig. 5a), also par for similar commercial product test outcomes. Both nitinol-based monofilament (Fig. 5b) and strand (Fig. 5d) constructs exhibited lower strength levels (about 30%) and much higher elasticity compared to 35N LT counterparts due to pseudoelastic strain recoverability. Elastic modulus under initial loading to about 200 MPa, prior to transformation onset, was reduced for the nitinol-based strand as compared to the wire (Fig. 5d vs. 5b). In monotonic tensile loading to fracture, the work energy to fracture averaged 23.7 and 65.9 mJ/mm^3 for 35NLT-DFT-28Ag and NiTi-DFT-30Ag respectively.

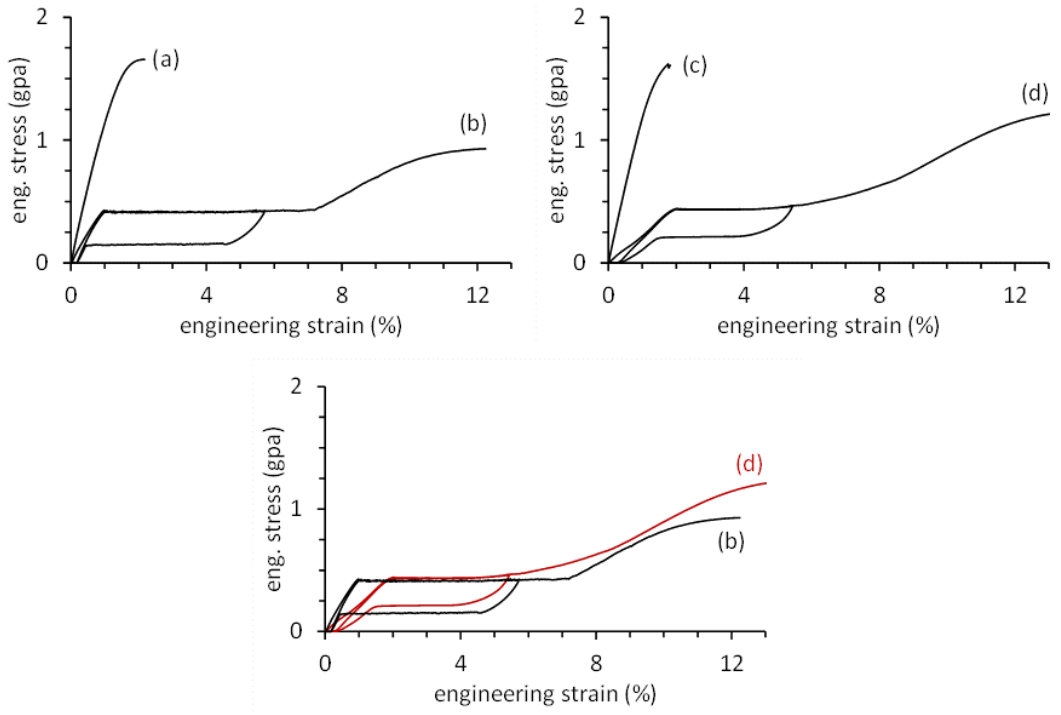

Figure 5 – Tensile stress-strain curves of materials (a) 0.1 mm 35NLT-DFT-28Ag wire; (b) 0.1 mm NiTi-DFT-30Ag wire; (c) 1x19x0.025; 0.125 mm 35NLT-DFT-28Ag strand; (d) 1x19x0.025; 0.125 mm NiTi-DFT-30Ag strand.

The results of DC resistance testing for the 1x19 strand configuration are given in Table 2 with similar mean values for either material. At a mean of 5.99 ohm/m, the NiTi-DFT was about 5% more conductive that the 35N LT-DFT stranded wire, consistent with the slightly larger core in the NiTi-DFT wire.

Table 2. DC Resistance test summary of stranded DFT wires.

	Strand Ø [mm]	Resistance [ohm/m]		Strand Ø [mm]	Resistance [ohm/m]
35N LT-DFT Stranded Wire	0.1288	6.32	NiTi-DFT Stranded Wire	0.1257	5.99
	0.1290	6.32		0.1255	5.98
	0.1288	6.32		0.1255	5.98
	0.1290	6.31		0.1257	5.98
	0.1285	6.33		0.1255	6.00
	0.1290	6.33		0.1255	6.00
mean	0.1289	6.32	mean	0.1256	5.99
SD	0.00021	0.0067	SD	0.00013	0.0089

Figure 6 shows the empirical probability of fracture as a proportion of 10 samples each of Wires 1 and 2 that fractured prior to the 10^8-cycle runout criterion in strain-based R = -1 rotating beam fatigue in 310K 0.9% saline solution. From zero to fifty percent probability of fracture the NiTi-DFT-30Ag wire showed a 90 to 100% increase in strain-load capability as compared to 35NLT-DFT-28Ag wire, which reached 100% probability of fracture at 0.5% while the nitinol had an equivalent fracture probability at 1.1% alternating strain.

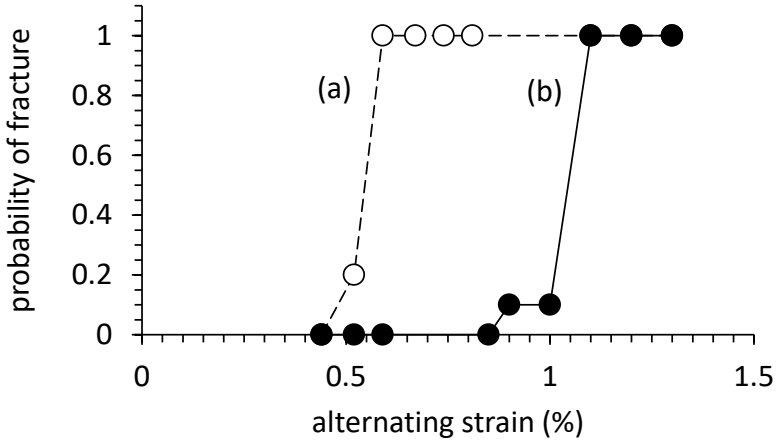

Figure 6 – Probability of fracture (N = 10) at less than 10^8 cycles in rotating beam fatigue testing of 0.1 mm wire. Probabilities were empirically derived from sample size 10 per alternating strain level at R = -1 strain load ratio for (a) Ø 0.1 mm 35NLT-DFT-28Ag wire and (b Ø 0.1 mm NiTi-DFT-30Ag wire.

Figure 7 shows fixtured bifilar coil samples from 35NLT-DFT-28Ag, and NiTi-DFT-30Ag before and after cycling. The initial 3.5 mm gaged grip separation is shown in panel a, and 200% structural strain extension to a mean 10.5 mm gage is shown in panel b, both for the 35N LT-based cohort. Panel c shows typical fracture of 35NLT-DFT-28Ag whereas panel d shows typical survival of NiTi-DFT-30Ag after more than 20 million cycles. Figure 8 provides a plot of empirical probability of fracture from N = 6 sampling of both material types. Bifilar 35NLT-DFT-28Ag wire survived to a total of 10^7 cycles at 10% structural strain cycling with five of six samples breaking in similar fashion to Figure 7c during cycling at 15% structural strain. In contrast, NiTi-DFT-30Ag showed zero fracture during 15% cycling whereas two of six samples survived to a total of 3 x 10^7 cycles during cycling at 21.4% structural strain.

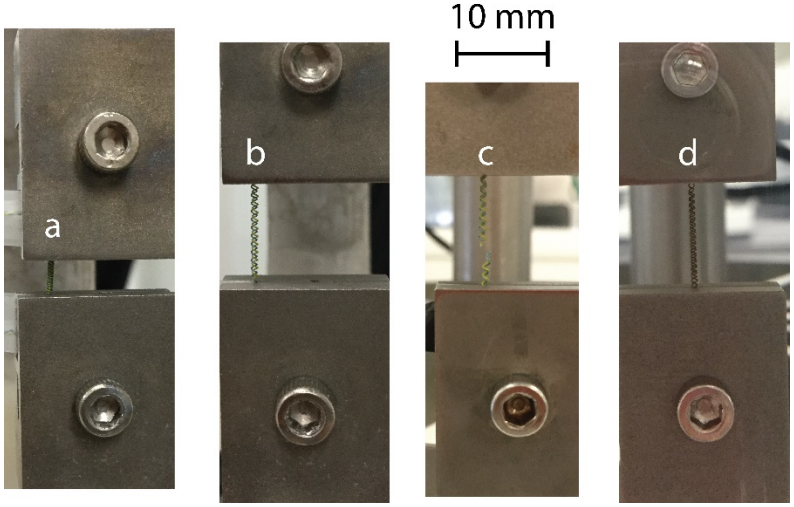

Figure 7 – Fixtured bifilar coil samples in situ to the tension-tension fatigue test device showing: (a) clamped sample at 3.5 mm gage length; (b) sample after extension to 200% macro structural strain (10.5 mm) mean condition; (c) fracture in bifilar 35NLT-DFT-28Ag characteristic of this cohort after 15% structural strain cycling to a total of 12 million cycles, and; (d) non-fracture in bifilar NiTi-DFT-30Ag in a sample from the NiTi-based cohort after 21.4% structural strain cycling.

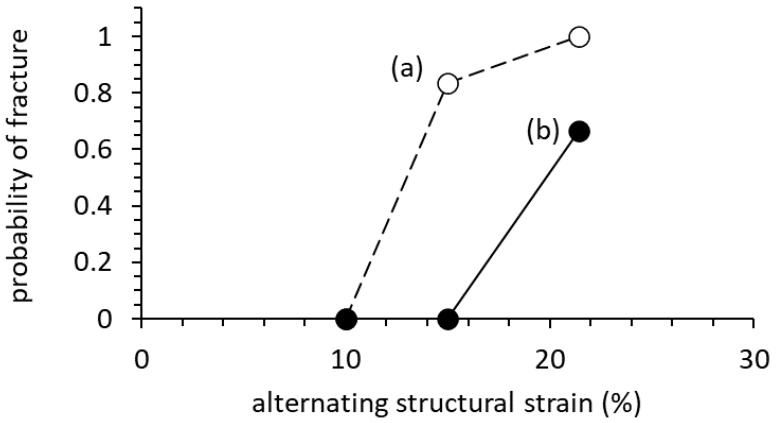

Figure 8 – Empirical probability of fracture at less than 10^7 cycles for bifilar 35NLT-DFT-28Ag (a) and NiTi-DFT-30Ag (b) conductors under coil-axial tension-tension fatigue at 200% mean structural strain and varied levels of structural strain conducted in 310 ± 2K distilled water.

Discussion

There may be significant device durability benefits available by the adoption of nitinol-based conductors into neurostimulation and cardiac stimulation applications. Nitinol-based conductor materials, such as NiTi-DFT®-30%Ag wire, can perform at higher strain-loading without fracture than conventional 35N LT-based systems by 50 to 100% based on lab bench results in coil and wire fatigue testing respectively (refer to Figures 5 and 7). The electrical resistivities of both nitinol (75-85 µohm-cm) and 35N LT (103 µohm-cm) based systems with and without silver core are comparable which should allow similar form and fit into wire-, coil-, strand- and cable-based designs.

A materials system capable of nitinol shape programming even with an electrically insulative layer may also enable new lead solutions. High temperature insulative coatings such as polyimide or PTFE may be used while enabling secondary or tertiary thermal shaping of leads to shapes that compliment anatomical placement. An improved lead for left ventricular stimulation through the coronary sinus (CS) in cardiac resynchronization therapy (CRT) may serve for illustrative discussion. Here, a CRT lead of polyimide-coated nitinol-silver could be heat programmed or shape set to a secondary helix or curve to compliment passive fixation in the CS enabling good passive anchoring and wall contact like a nitinol-based self-expanding vascular stent. Perhaps such technology could help alleviate adverse issues such as lead dislodgement and CS dissection, or to provide more durable multifunctional leads [15, 16] by providing gentle but thorough wall apposition in a device with improved delivery navigation and deployment.

As with any material design strategy, there are potential tradeoffs to nitinol-based implantable conductors versus their 35N LT counterpart. For one, while nitinol is widely used in implantable peripheral vascular devices, it has not yet served in implantable stimulation, to the authors' knowledge. Another tradeoff is that the ultimate strength of nitinol is typically lower than 35N LT DFT® wire by about 30%, but the material is also able to absorb more strain-energy due to its compliance and superelasticity (refer to Figure 5, a-d). The high compliance and resilience of nitinol-based conductor systems may enable easy absorption and dissipation of mechanical handling, anchoring and in-service stresses without fracture risk.

Conclusion

Wire-based subcomponents with a high conductivity silver core were designed, produced, and characterized with the following takeaways:

- Nitinol is effectively substituted for 35N LT with 50 to 100% improvements in lab bench strain-fatigue performance for bifilar coils or monofilament wire at body temperature.
- Electrical isolation of polyimide coating of the nitinol-based conductors is visually maintained after high temperature (450-550°C) secondary shape setting.
- The DC resistance of 1x19x0.025; 0.125 mm 35N LT-DFT-28Ag (6.32 ohm/ft) and NiTi-DFT-30Ag (5.99 ohm/ft) are similar.
- The ultimate strength of the NiTi-DFT-30Ag wire at about 1000 MPa was lower than 35NLT-DFT-28Ag wire at about 1600 MPa.
- Despite lower strength, the tensile fracture energy was more than 150% greater for nitinol-based conductor at 65.9 mJ/mm^3 for NiTi-DFT-30Ag and 23.7 mJ/mm^3 for 35NLT-DFT-28Ag.

These characterization data may lead to creative design enhancement of future sensing and stimulation subcomponents where nitinol-based conductors may give more durable sensing and stimulation performance over long term implant service under mostly displacement-controlled fatigue load conditions.

Acknowledgements

The authors wish to thank J. Topp, G. Archambault and R. Bow for assistance in multifilament strand and coil builds; S. Mitchell and A. Henry for metallographic preparation; S. Telley and C. Reinhard for coating process design and execution; and finally, FWM Staff for funding this research. Author JE Schaffer thanks C. Chao (Element Materials Technology) for valuable assistance in tension-tension fatigue fixture design and execution.

References

[1] J. Gardner, "A history of deep brain stimulation: Technological innovation and the role of clinical assessment tools," *Social studies of science,* vol. 43, no. 5, pp. 707-728, 2013.

[2] G. Van Welsenes, C. Borleffs, J. Van Rees, J. Atary, J. Thijssen, E. Van der Wall and M. Schalij, "Improvements in 25 years of implantable cardioverter defibrillator therapy," *Netherlands Heart Journal,* vol. 19, no. 1, pp. 24-30, 2011.

[3] E. Papasteriadis and P. Margos, "Pacing and sensing of human heart for over 31 years with the same apparatus (generator and lead)," *Case reports in cardiology,* 2015.

[4] D. Fisher and H. Czech, "Conductive catheter". U.S. Patent 3,416,533, 17 Dec 1968.

[5] R. Jones, H. Lippard, T. Stephenson, R. Myers and D. Bradley, "Cobalt-nickel-chromium-molybdenum alloys with reduced level of titanium nitride inclusions". U.S. Patent 8,048,369, 1 Nov 2011.

[6] J. E. Schaffer, "A probabilistic approach to modeling microstructural variability and fatigue behavior in ASTM F562 medical grade wire," in *Proceedings of the 9th International Congress on Fatigue, Fatigue 2006*, Atlanta, GA, 2006.

[7] J. Schaffer, A hierarchical initiation mechanism approach to modeling fatigue life variability in 35Co-35Ni-20Cr-10Mo alloy medical wire, West Lafayette, IN: Purdue University Dissertation, 2007.

[8] J. Schaffer, "Fatigue damage resistant wire and method of production thereof". U.S. Patent 8,840,735, 23 Sep 2014.

[9] J. Schaffer, *Unpublished internal laboratory developed fatigue data,* Fort Wayne: Fort Wayne Metals Research Products Corp, 2008.

[10] A. Foster, Interviewee, *On opportunities for materials enhancements for future generation lead systems.* [Interview]. 11 April 2018.

[11] C. D. Schuger and et al., "Ventricular lead transection and atrial lead damage in young softball player shortly after the insertion of a permanent pacemaker," *Pacing and Clinical Electrophysiology,* vol. 15, no. 9, pp. 1236-1239, 1992.

[12] R. G. Hauser and et al., "Early failure of a small-diameter high-voltage implantable cardioverter-defibrillator lead," *Heart Rhythm,* vol. 4, no. 7, pp. 892-896, 2007.

[13] G. H. Crossley and et al., "Extraction of chronically implanted coronary sinus leads active fixation vs passive fixation leads," *Heart Rhythm,* vol. 13, no. 6, pp. 1253-1259, 2016.

[14] J. E. Schaffer and R. Gordon, "Engineering characteristics of drawn filled nitinol tube," in *Proceedings of the International Conference on Shape Memory and Superelastic Technologies*, Materials Park, OH, 2004.

[15] J. J. Bax, T. Abraham, S. S. Barold, O. A. Breithardt, J. W. Fung, S. Garrigue, J. Gorscan III, D. L. Hayes, D. A. Kass, J. Knuuti, C. Leclercq, C. Linde, D. B. Mark, M. J. Mohaghan, P. Nihoyannapoulos, M. J. Schalij, C. Stellbrink and C.-M. Yu, "Cardiac resynchronization therapy: Part 2 - Issues during and after device implantation and unresolved questions," *Journal of the American College of Cardiology,* vol. 46, no. 12, pp. 2168-2182, 2005.

[16] L. Dong, A. B. Closson, C. Jin and Y. Nie, "Multifunctional pacemaker lead for cardiac energy harvesting and pressure sensing," *Advanced healthcare materials 9.11,* p. 2000053, 2020.

[17] J. E. Schaffer, "Structure-property relationships in conventional and nanocrystalline NiTi intermetallic wire," *Journal of materials engineering and performance,* vol. 18, no. 5, pp. 582-587, 2009.

[18] A. R. Pelton, D. Stoeckel and T. W. Duerig, "Medical uses of nitinol," *Materials science forum,* vol. 327, 2000.

[19] A. R. Pelton, V. Schroeder, M. R. Mitchell, X.-Y. Gong, M. Barney and S. W. Robertson, "Fatigue and durability of Nitinol stents," *Journal of the mechanical behavior of biomedical materials,* pp. 153-164, 2008.

[20] T. Duerig, A. Pelton and D. J. Stoeckel, "An overview of nitinol medical applications," *Materials Science and Engineering: A 273,* pp. 149-160, 1999.

[21] V. M. Marrey, R. Burgermeister, R. B. Grishaber and R. O. Ritchie, "Fatigue and life prediction for cobalt-chromium stents: a fracture mechanics analysis," *Biomaterials 27.9,* pp. 1988-2000, 2006.

[22] J. E. Schaffer, "A probabilistic approach to modeling microstructural variability and fatigue behavior in ASTM F562 medical grade wire," in *Proceedings of the 9th International Congress on Fatigue*, Atlanta, Georgia, 2006.

[23] R. S. Porter, T. Kanamoto and A. E. Zachariades, "Property opportunities with polyolefins: a review. Preparations and applications of high stiffness and strength by uniaxial draw," *Polymer,* vol. 35, no. 23, pp. 4979-4984, 1994.

[24] J. E. Schaffer, "DFT biocompatible wire," *Advanced materials & processes,* vol. 16, no. 10, pp. 51-54, 2002.